Title : will be set by the publisher
Editors : will be set by the publisher
EAS Publications Series, Vol. ?, 2004

AN X-RAY VIEW OF RADIO SOURCES

D. A. Schwartz[1]

Abstract. We review recent examples where the synergy between radio and X-ray observations has led to substantial progress in understanding astronomical systems. The sub-arcsecond imaging capabilities of the *Chandra* X-ray observatory provides a 100-fold improvement for comparing X-ray and radio structures. We specifically discuss examples which provide insight into the outflow of material and energy from pulsars and supernovae, the centers of clusters of galaxies, and the nuclei of quasars.

1 Introduction

In the X-ray band, as in the radio region, one studies virtually every type of astronomical system. Both channels are good indicators of non-thermal activity, and of the beginnings and ends of the lifecycle of stars and massive black holes. In the early days of X-ray astronomy, when locations of sources were no more precise than the order of a square degree, the coincidence of a strong radio source in the region served as an argument for the X-ray identification, for example, M87 (Bradt *et al.* 1967) and 3C 273 (Bowyer *et al.* 1970).

As a theme for this review, I will concentrate on systems where the X-ray and radio observations are telling us about the outflow of material and energy. This is in contrast to what might be called "classical" X-ray astronomy, which studied accretion processes. Infall of gas not only explained the energy source, but also led directly to the calculations of X-ray emission from disks in galactic neutron star, black hole, and white dwarf binaries. Accretion onto supermassive black holes was inferred to power quasars and Active Galactic Nuclei (AGN). In these cases the X-ray and non-thermal optical continuum are most closely related. If accretion disks were the only setting for X-ray emission, there might be few X-ray and radio connections, as the peak radiation frequency corresponds to the temperature in the innermost disk, and therefore does not span the very broad range from $\approx 10^9$ Hz radio emission to $\approx 10^{18}$ Hz X-ray emission.

[1] Harvard/Smithsonian Center for Astrophysics, Cambridge, MA 02138, USA

DOI: (will be inserted later)

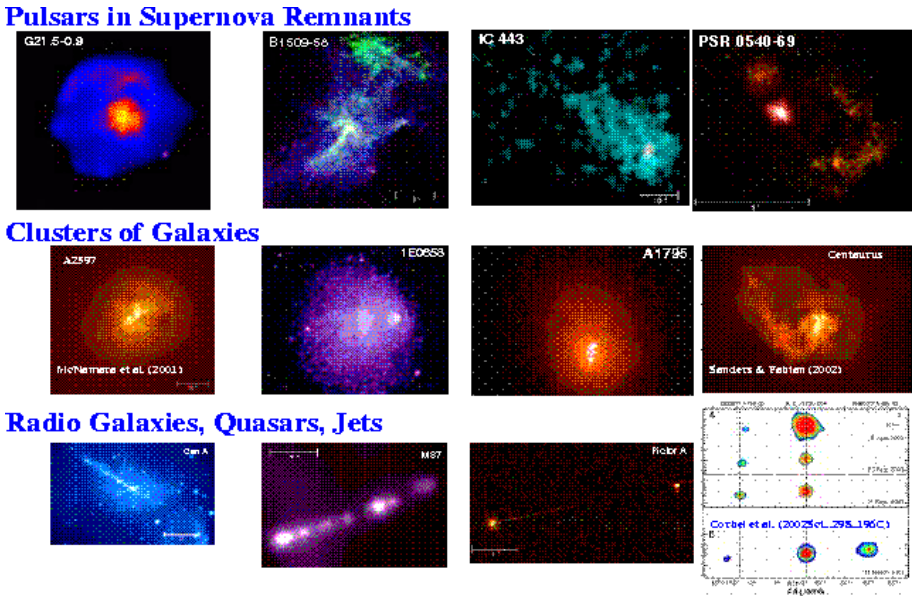

Fig. 1. *Chandra* images of examples of the systems discussed in this review. Credits: NASA/MSFC/SAO/CXC (top row, middle row, left 3 on bottom row); Corbel *et al.* 2002 (bottom row right).

Figure 1 provides examples of systems representing the three topics I will discuss: pulsars and supernova remnants; cooling flows in clusters of galaxies; and jets in quasars and radio galaxies.

In clusters of galaxies, the X-ray emission from the hot gas filling the volume between the galaxies was shown to have temperatures consistent with the gravitational potential of the cluster. In a substantial fraction of clusters, the gas was observed to be sufficiently dense that it would cool in much less than a Hubble time, and it was interpreted that massive cooling flows involving hundreds of solar mass per year were condensing onto the cluster centers (Arnaud (1988), Fabian (1994)). This created a great puzzle, as neither the destination of the cooling gas, nor great quantities of gas at temperatures less than 1 to 2 keV have been found. It now appears that powerful radio sources in cD galaxies in the cluster cores (Burns (1990)) provide the energy to offset the cooling.

In contrast to accretion, a major theme of radio astronomy has been the origin of cosmic rays, the acceleration of particles to ultra high energies, and the transport of energy in jets to distances of pc to Mpc away from the nuclei of active galaxies. Radio astronomy has been primarily an imaging rather than spectroscopic science (with some important exceptions which we have heard at this symposium). In this article I therefore emphasize X-ray imaging. For decades radio observations have studied detailed structure in supernova remnants, emission from cluster of galaxies and sources in clusters, and jets in active galaxies. With the half-arcsecond X-

ray imaging now available from the *Chandra* X-ray Observatory, we can finally compare X-ray with GHz radio observations on the same angular scales.

We adopt a flat, accelerating cosmology with Hubble constant H_0=70 km s^{-1} $Mpc,^{-1}\Omega_m$=0.3, and Ω_Λ=0.7.

2 Pulsars and Supernova Remnants

From the earliest radio observations of pulsar periods, and of the rates at which the periods were increasing, it was found that from 10^{35} to 10^{39} erg s^{-1} of rotational energy was being lost. The radio luminosities were typically orders of magnitude smaller, and even in those cases with X-ray emission, such as the Crab Nebula and Vela Pulsar (Fig. 2), the total radiated luminosity was a very small fraction of the energy loss. It was presumed that the balance went into relativistic particles (Michel (1969a)) and driving a wind (Michel (1969b)). In some cases, a plerion, or pulsar wind nebula, was present, and interpreted as the manifestation of the outflow. The picture was that a cold, relativistic gas was driven away from the speed of light cylinder. This gas would not be directly detectable, until it formed a shock where it encountered the nebular gas. Gaensler (2003) gives an excellent review of all these issues.

We now see this termination shock in the Crab and Vela as indicated in Figure 2. The figure shows rings indicating equatorial flow, and jets. The jets must be along the rotational axis, and not the magnetic pole, since the latter must sweep a wide cone on the sky, giving pulses when it intersects our line of sight. These pulsars give us a clear case of a jet which is associated with rotation.

Figure 3 (from Pavlov *et al.* 2003), shows a sequence of X-ray images of the outer jet in the Vela Pulsar Nebula, over an 8 month time interval. There are

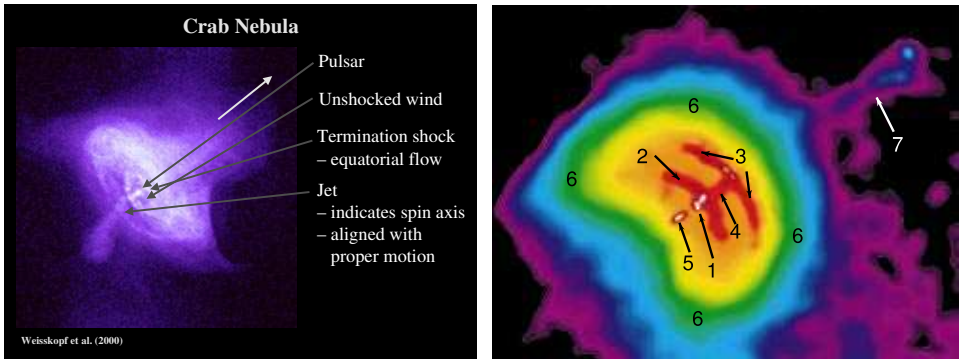

Fig. 2. *Chandra* images of the Crab Nebula (left, NASA/CXC, from Weisskopf *et al.* 2000) and the Vela Pulsar Nebula (right, from Pavlov *et al.* 2003). The large arrow on the left shows the direction of the spin axis and the proper motion, for *both* pulsars. Numbered regions in Vela indicate 1. pulsar; 2. termination shock; 4. and 5. the inner jet and counterjet, respectively; 7. the outer jet.

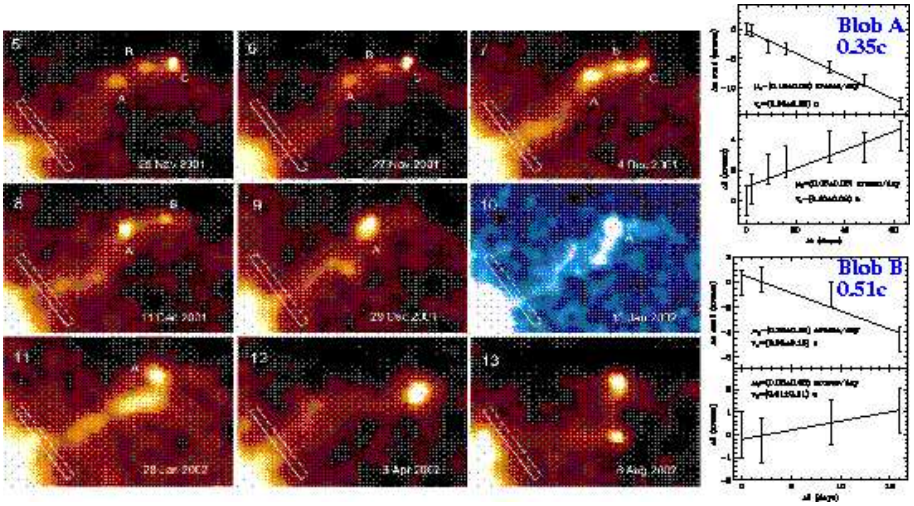

Fig. 3. Time sequence of the outer Vela jet (Pavlov *et al.* 2003), showing remarkable changes in morphology, and apparent relativistic motion of blobs. Image 10 is with the HRC, the others are with ACIS S3.

distinct morphological and brightness changes, e.g., in as few as 7 days from 4 to 11 December, 2001. These changes are attributed to magnetic instabilities in the jet, and/or its interaction with the interstellar medium.

Figure 3 (right column) plots the position vs. time for two of the knots, "A" and "B" relative to the narrow rectangle which is superposed in fixed celestial coordinates in the images. At the distance of the Vela pulsar, 300 pc, these motions respectively correspond to 0.35 and 0.51 times the velocity of light. The changing image may be due to moving material or to moving patterns in the jet.

Figure 4 (from Gaetz *et al.* (2000), figs 5. and 6.) shows the supernova remnant 1E 0102.2-7219 in the Small Magellanic Cloud (SMC). It is a young, oxygen rich remnant, which has been observed repeatedly since orbital activation as a calibration target. Flanagan *et al.* (2000), and Fredericks *et al.* (2001) discuss HETG observations which show details of the X-ray line ionization structure and velocities. Gaetz *et al.* (2000) discuss how the X-ray picture shows for the first time the sharp interaction of the the outgoing shock with the interstellar medium, delineated by the outer edge of the X-ray gray-scale image to the left. The most intense X-ray ring is the reverse shock, moving back into the expanding medium. The radio emission is brightest in the region between the two shocks, with the interpretation that the shocks are intensifying the magnetic fields, and accelerating the particles.

The composite supernova remnant Kes75 is discussed by Helfand *et al.* (2003) (figure 5). The false-color X-ray image in the left panel shows the shell structure of the outer shock, the peak X-ray intensity consistent with a reverse shock, and

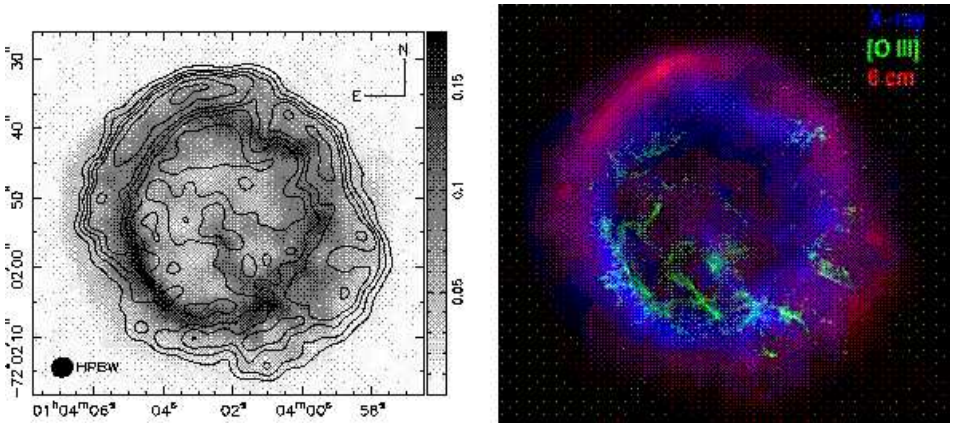

Fig. 4. Left Panel (Figure 5 from Gaetz *et al.* (2000)): X-ray (gray scale) and radio (contours) images of the supernova remnant E0102-72 in the SMC. Right Panel (Figure 6 from Gaetz *et al.* (2000)): X-ray (blue), 6 cm (red) and optical [O III] emission (green).

the 20 cm VLA radio emission from the outer, shocked X-ray emitting regions, all as in E0102-72. There is also a radio and X-ray bright central nebula, for which their expanded image (top center) shows a synchrotron nebula, a pulsar, and hot spots to the NNE and SSW which might be from a jet. Helfand *et al.* (2003) analyze the spectrum of the pulsar, and the nebula, separately, and show they are continuous, non-thermal emission, which they attribute to synchrotron radiation (figure 5, top right panel). Perhaps their most interesting discovery is in the X-ray spectrum of a broad region of the shell remnant, shown in the lower right. While lines of Mg, Si, and S are clearly present, and require a hot gas, no purely thermal emission model (indicated by the histogram) can provide both the line emission and all the continuum emission up to the 7 keV plotted in the figure. They model a combination of a thermal and a synchrotron spectrum, where the latter is due to a dust halo scattering the X-ray emission from the pulsar and its synchrotron nebula.

3 Cooling Flows in Clusters of Galaxies

The *Chandra* calibration observation of the Hydra A cluster of galaxies is shown in figure 6 (from McNamara *et al.* (2000) and Nulsen *et al.* (2002)). Hydra A had been inferred to have a large cooling flow, of order 250 solar masses per year (White *et al.* (1997)). However, only of order 10 solar mass per year could be accounted for by star formation rates (McNamara (1995), Hansen *et al.* (1995)). A general suggestion to prevent cooling flows condensing in cluster centers was that radio sources in the central cD galaxy provided the energy to balance the radiation loss (cf. Tucker & Rosner (1983)). A convential picture was that the

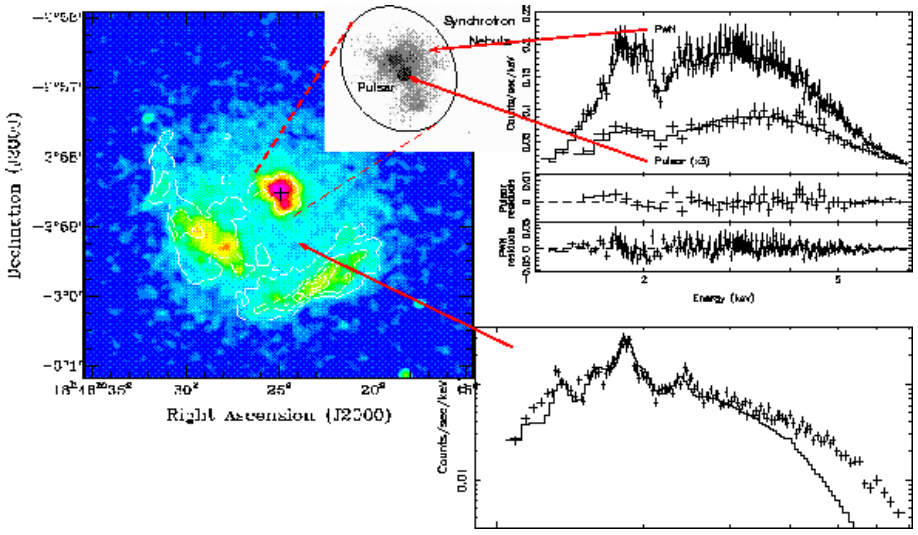

Fig. 5. The composite supernova remnant Kestevan 75 (adapted from Figures 1, 2, 3, and 7 of Helfand *et al.* (2003)). Left panel: False color X-ray image with 20 cm radio contours. Top center: X-ray image of the pulsar and synchrotron nebula. Right panels: X-ray spectra of the pulsar, synchrotron nebula, and a region of the shell inside the shock.

radio plasma was emitted in a jet, which generated a shock upon colliding with the cluster gas (Clarke *et al.* (1997), Heinz *et al.* (1998)).

The left panel of Figure 6 was discussed by McNamara *et al.* (2000), who emphasized the coincidence of the apparent "cavity" in the X-ray emission (gray scales in top and bottom panels) with the 6 cm VLA emission (contours in bottom panel, from Taylor *et al.* (1990)). However, as shown in the temperature map of the cluster by Nulsen *et al.* (2002), (right panel), the higher density gas surrounding the cavities is at a *lower* temperature than the more distant cluster gas, and thus is not the result of a strong shock. This leads to the interpretation that the "cavity" is actually a buoyantly rising "bubble."

We can use the X-ray observations to learn much about the conditions in cluster cores in general. We can measure, as a function of position, the electron temperature, T, from the shape of the X-ray spectrum, and the density n_e from the measured intensity, which is proportional to $n_e^2\sqrt{T}$. The coincidence of the X-ray cavities with the radio emission gives us three more relations: The work, $p\Delta V$, done to create the cavity should equal the energy available from the radio jet; the pressure of the radio plasma should approximately balance the X-ray gas pressure at the cavity boundaries; and the time scale for the bubble to rise and expand, gives lifetimes. In particular, both the observation that the bubbles do not expand faster than the sound speed (due to lack of strong shocks), and the estimate that they rise with a velocity of order the Keplarian velocity at their

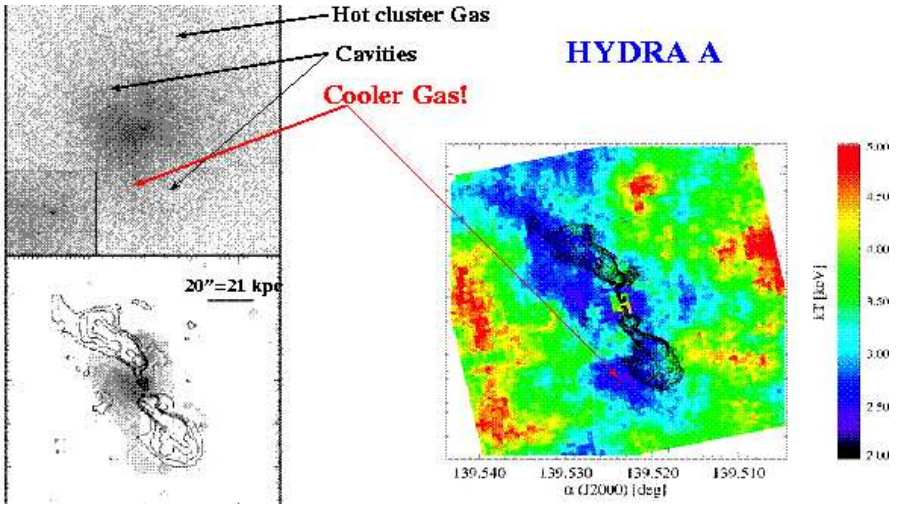

Fig. 6. X-ray (gray scale and false color) image and 6 cm contours of the central region of the Hydra A cluster. (Left, from McNamara *et al.* (2000); right from Nulsen *et al.* (2002).)

position (Churazov *et al.* (2000)), leads to velocities of order hundreds of km/s, and ages of a few 10^7 years.

In the case of Hydra A, Nulsen *et al.* (2002) estimate $p\Delta V \approx 1.2 \times 10^{59}$ ergs, while if one assumes the magnetic field and particles in the radio plasma have a minimum energy density (which is very nearly the equipartition value) this density times the volume is only $u_{me}\, V \approx 1.4 \times 10^{58}$ ergs. On the other hand, based on the rotation measure, Taylor *et al.* (1990) argue that the magnetic field is several times less than the equipartition value, and if so the energy in the radio plasma could be comparable to the work done creating the cavities.

The remarkable original discovery of cluster gas cavities coincident with radio emission was made by Böhringer *et al.* (1993) using *ROSAT* high resolution imager observations of the Perseus Cluster. This cluster contains the powerful radio source 3C 84. The original *Chandra* observations are shown in Figure 7, from Fabian *et al.* (2000) (left panels) and Fabian *et al.* (2002) (right panels). We see the original cavities, (also called "holes"), within about 10 kpc nearly N and S of the cluster center. *Chandra* data shows that the X-ray bright rims of the holes are *cooler*, about 2.7 keV, than the extended cluster emission which is at about 6.5 keV (Fabian *et al.* (2000)). As in the case of Hydra A, the cavities therefore could not be interpreted as shock heating by the radio plasma as predicted, e.g. by Heinz *et al.* (1998).

The work to evacuate the North cavity is about $p\ \Delta V \approx 2 \times 10^{58}$ ergs. A standard minimum energy calculation, which takes a filling factor ϕ=1 and a ratio of proton to electron energy density k=0, gives $u_{me}\, \Delta V \approx 4 \times 10^{56}$ ergs,

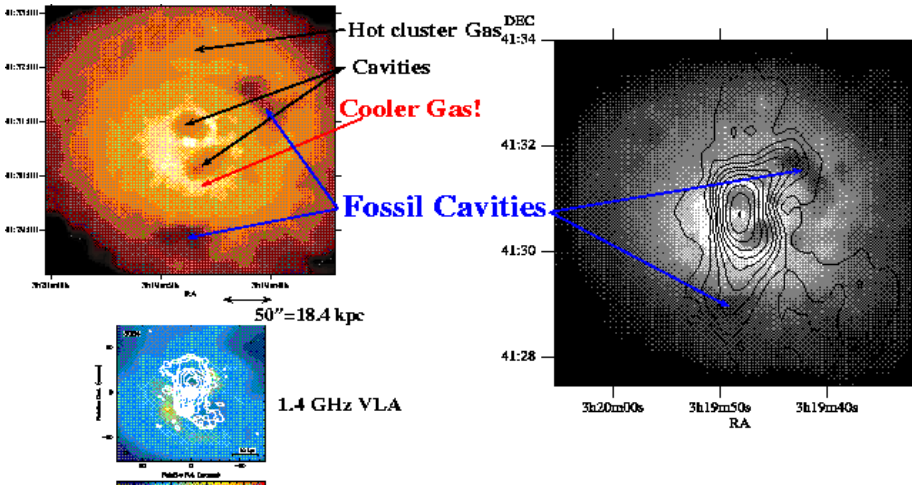

Fig. 7. Left panels (from Fabian *et al.* (2000), figs. 5 and 7): False color X-ray image of the center of the Perseus cluster, showing the inner X-ray cavities filled with 1.4 GHz emission. Right panel (from Fabian *et al.* (2002), Fig. 3): gray scale X-ray image, showing the 74 MHz radio contours extending to the outer "fossil" cavities.

almost a factor of 100 smaller. Fabian *et al.* (2002) use this to infer that the ratio $\frac{k+1}{\phi}$ is of order 600, and at least 180 to establish pressure equality, all under conditions of minimum energy. On the contrary, in order that the synchrotron lifetime of the electrons emitting at 1.4 GHz be longer than the age of the N cavity, Fabian *et al.* (2002) find that the magnetic field is 4 to 10 times less than equipartition value, (which also requires $\frac{k+1}{\phi} < 500$).

The regions of lower surface brightness 1.′5 to the NW and 2′ to the S, are interpreted by Fabian *et al.* (2002) as due to bubbles for which the high frequency emission is absent due to ageing of the radio electrons. They argue that the 74 MHz radio images (Blundell *et al.* (2002)) which point to these "fossil" or "relic" cavities, trace earlier radio jets which evacuated and energized these regions.

The mechanism by which the central, active radio source provides the energy to balance the cooling flow may have been seen directly in a 200 ks observation of Perseus A (Fabian *et al.* (2003)). They explore the possibility that faint X-ray intensity ripples (seen in their Figure 3.) are sound waves moving out from the interaction of the jets producing the bubbles. Since they do not detect any temperature variations in these regions, density oscillations most economically explains the intensity variations. They invoke viscosity to dissipate the sound energy into the required heating of the gas.

The lesson of all the bubbles in X-ray clusters (e.g., Blanton *et al.* (2001), McNamara *et al.* (2001), Sanders & Fabian (2002), Sun *et al.* (2003)) is that the central black hole must be producing much more energy than we see from the direct radio emission or from the minimum energy arguments. It is therefore likely that a

central active galaxy produces the energy output needed to counteract the cooling flows. Nulsen (2003) argues that this proceeds via a feedback process, whereby the central AGN becomes more active whenever the cooling gas can effectively accrete to the central black hole, and the increased activity then retards or stops the cooling flow.

4 Jets in Radio Galaxies and Quasars

X-ray jets in a diverse collection of objects has become possible as a distinct field of research only with the 100-fold improvement in 2-dimensional imaging afforded by the 0.″5 resolution of *Chandra*, compared to the previous 5″ imaging of the *Einstein* and *ROSAT* observatories. Jets are studied in contexts as varied as the symbiotic binary R Aqr (Kellogg *et al.* (2001)), the galactic black hole candidate XTE J1550-564 (Corbel *et al.* 2002), plerions (discussed in Section 2), low power FR I sources where the X-ray emission is interpreted as an extension of the radio synchrotron emission (e.g., Worrall *et al.* (2001)), and in powerful FR II galaxies and quasars. This section will consider only the last topic.

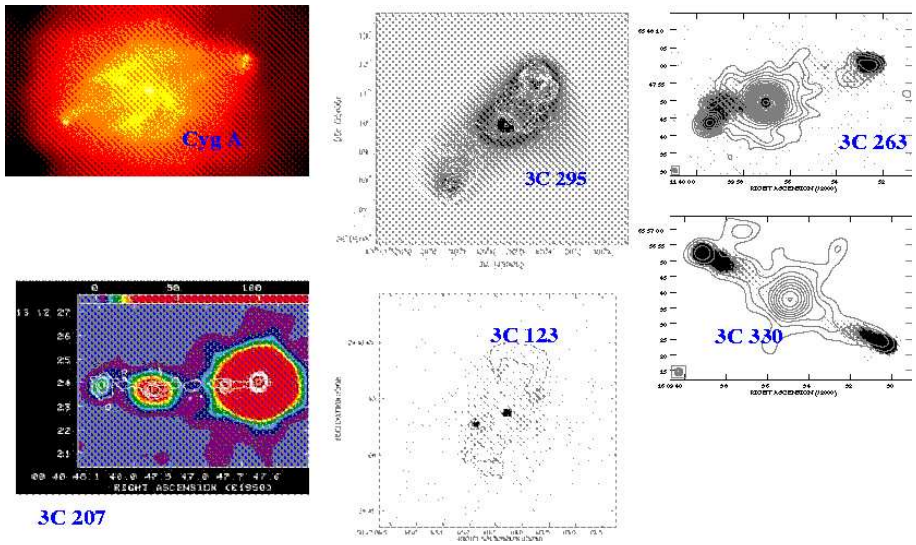

Fig. 8. X-ray hotspots (false color and gray scale) at the end of radio jets (contours). Clockwise from upper left: Cygnus A (from Wilson *et al.* (2000)), 3C 295 (from Harris *et al.* (2000)), 3C 263 and 3C 330 from Hardcastle *et al.* (2002)), 3C 123 (from Hardcastle *et al.* (2001)), and 3C 207 (from Brunetti *et al.* (2002)).

In Figure 8 I select some examples which illustrate the X-ray emission at the hotspots at the end of jets. In all these cases, from the radio observation of flux and spatial extent, plus the assumption of equipartition, one can conclude that the synchrotron photon density is the largest energy density in the X-ray emitting

region. Thus the natural X-ray mechanism is synchrotron self-Compton (SSC) emission. The X-ray fluxes are generally consistent with magnetic fields in the range 70 to 320 μGauss, which are just a little below the equipartition field values (see refs. given in figure caption). This is a body of evidence that conditions near equipartition might be a reasonable assumption.

Figure 9 shows some of the X-ray images of jets (in false color), overlaid with radio contours. These are samples from two surveys, one by Sambruna *et al.* (2002), the other by Marshall *et al.* (2002), (also reported in Schwartz *et al.* (2003)). We also see the discovery image of PKS 0637-752 (Schwartz *et al.* (2000), and a radio-optical-X-ray view of the jet in 3C 273 (Marshall *et al.* (2001)). The X-ray emitting regions closely follow the radio in general, but the intensities sometimes correlate closely, as in the straight western jet of PKS 0637-752, and sometimes anti-correlate as in 3C 273. We will use the four PKS objects from our survey (bottom of Figure 9) to discuss the physical conditions in jets (Schwartz *et al.* (2003b)).

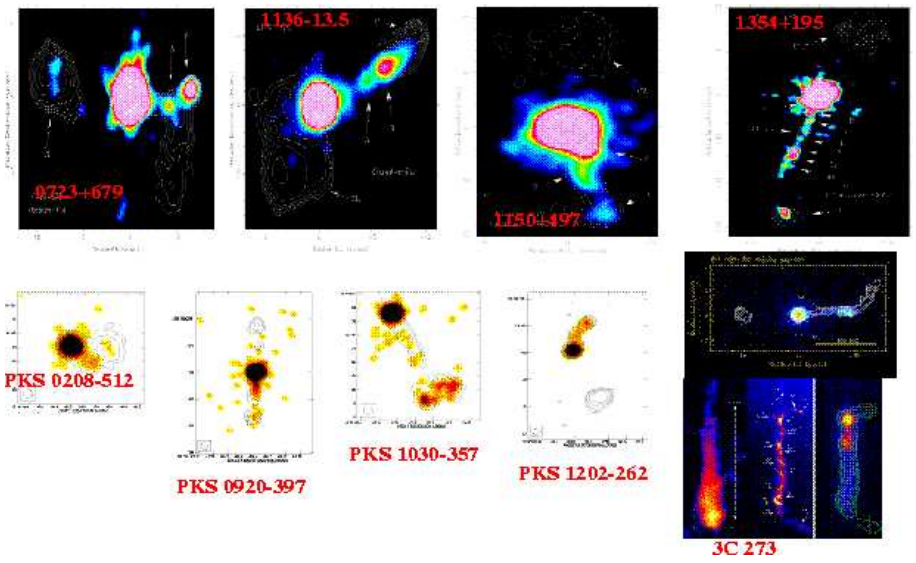

Fig. 9. Chandra images of X-ray jets. Top panel from Sambruna *et al.* (2002). Bottom: PKS objects from Schwartz *et al.* (2003b); PKS 0637-752 from Schwartz *et al.* (2000); 3C 273 from Marshall *et al.* (2001)

We have 8.64 GHz ATCA images of all our sources, and in some cases 4.8 GHz data. We smooth both the radio and X-ray to a $1\farcs2$ resolution, and superpose them by forcing coincidence of the quasar cores. We then divide the jets into distinct regions. This is somewhat subjective, guided by the features in the radio and X-ray emission. To label the different regions we use the term "knots" (K), with numbers increasing away from the quasar, but we don't intend this to prejudice the nature of the actual structure.

Figure 10 shows the spectral energy distributions we construct for each region.

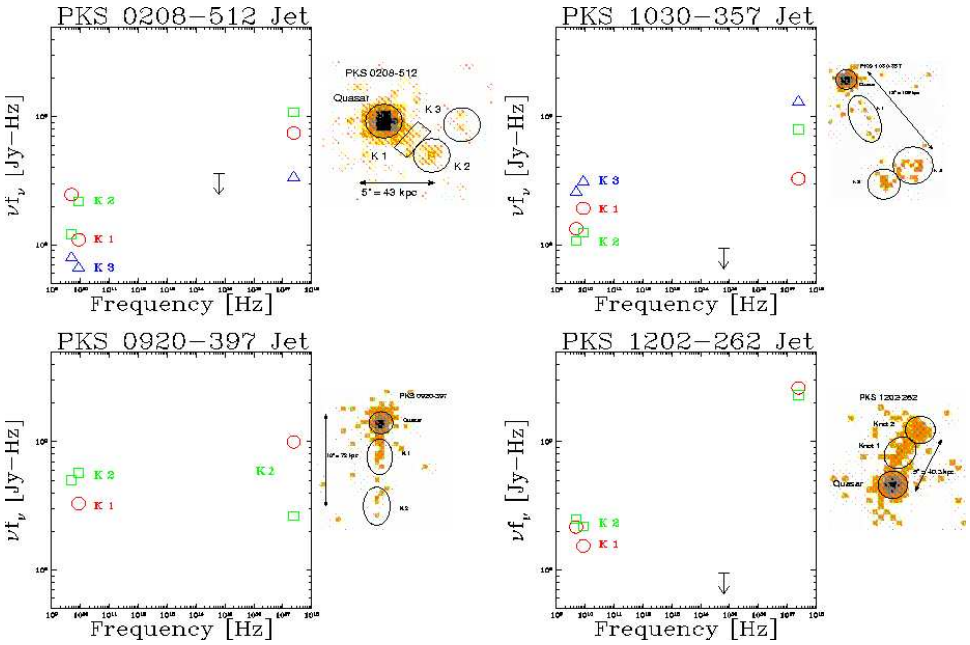

Fig. 10. Spectral energy distributions of regions within the X-ray jets.

Optical upper limits from Magellan observations (J. Gelbord, private communication and in preparation 2004) directly show that for most cases the X-ray emission cannot be a simple extension of the radio synchrotron spectrum. For other regions, e.g., K3 of PKS 0208-512, the radio spectral shape would not connect to the X-ray region. For some other regions, e.g., K2 of PKS 0920-397 and K2 of PKS 0208-512 the X-ray emission could well result from a continuation of the relativistic electrons to high enough energy to emit X-ray synchrotron emission, as inferred for the first knot, A1, in 3C 273 (Marshall *et al.* (2001)). The simplest X-ray emission mechanism, given the strong correlation with the radio, should invoke radiation from the same spectrum of relativistic electrons. This indicates some form of inverse Compton (IC) emission. From the size and radio emission, we know that SSC will not be important, and at 10's to 100's of kpc from the quasar the energy density of photons from the central black hole will not give significant radiation.

The most likely target photons for IC emission are the cosmic microwave background (CMB). This was originally discussed by Felten & Morrison (1966) in the context of explaining the cosmic X-ray background. However, in the original case of PKS 0637-752, calculating the equipartition magnetic field gave a result about 100 times larger than the maximum magnetic field which would allow the X-rays to be produced by IC/CMB radiation. The problem of requiring total energies more than 10^3 times larger was resolved by Tavecchio *et al.* (2000) and Celotti *et al.* (2001), who considered the enhancement of the apparent CMB density by the factor Γ^2,

(Dermer & Schlickeiser (1994)), in a frame moving with bulk relativistic velocity $\beta = \sqrt{(}1 - 1/\Gamma^2)$ with respect to the CMB frame. If one plots the required relativistic beaming factor $\delta = (\Gamma(1 - \beta\cos\theta))^{-1}$ against the required rest frame magnetic field, then since $\delta \propto B_{IC}$ and $\delta \propto 1/B_{eq}$, one can always find a solution for δ and B for which the source is near equipartition in its rest frame, and the same population of electrons produces radio synchrotron radiation in the B field, and X-ray inverse Compton radiation off the cosmic microwave background.

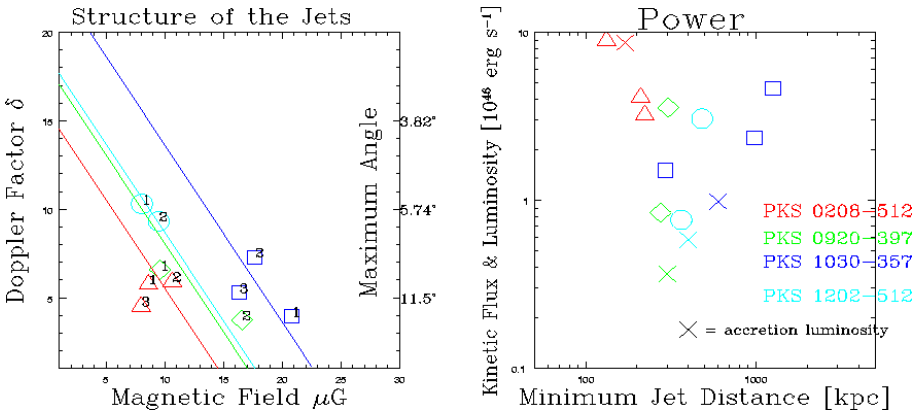

Fig. 11. Structure of the X-ray jets. Left panel shows the Doppler factors and rest frame magnetic fields inferred for each region. Uncertainties are systematics dominated and about a factor of 2. Solid lines show the loci of constant kinetic flux. Right panel plots the kinetic flux through each region, vs. the minimum space distance of each component. Colored triangles, diamonds, circles and squares indicate the same source in each frame. Crosses plot the bolometric radiative luminosity of the quasar.

We will continue by assuming all the jet emission is due to IC/CMB. Figure 11 (left panel) shows the range of Doppler factors, $\delta \approx 2$ to 10, and intrinsic magnetic fields, B ≈ 5 to 25 μG, for these objects (Schwartz *et al.* (2003b)). In this derivation, we have had to assume that $\Gamma = \delta$, since we do not have independent information on the orientation of the jet. From δ, we can infer a maximum angle of the jet from our line of sight, $\theta_{max} = \cos^{-1}[(\delta - 1/\delta)/\sqrt{(}\delta^2 - 1)]$, which we use to compute the minimum space distance (3 dimensions) of each region from the central quasar. We estimate (right panel of Figure 11) the kinetic flux of each element as $A\Gamma^2 cU$ (e.g., Ghisellini & Celotti (2001)), where A is the cross sectional area (and we assume cylindrical symmetry), and U the total energy density in the rest frame of the jet. We assume equipartition, with an equal energy in protons and electrons, so that U=3 $B^2/(8\ \pi)$. Under all these assumptions, the lines $\delta \propto 1/B$ are the lines of constant kinetic flux, as shown in the left panel.

In the right panel, the crosses plot the bolometric radiative luminosity of the quasar cores. We see that the kinetic flux in the jet is comparable to or greater than the accretion flux. This is consistent with the conclusion of Meier (2003) that

accretion flow models must also consider jet production.

One of the most dramatic implications of the inference that we see IC/CMB X-radiation from radio jets is that any given object would appear to have a constant X-ray surface brightness even as it were displaced to an arbitrarily large redshift (Schwartz (2002)). This is because the energy density of the CMB increases as $(1+z)^4$, exactly offsetting the $(1+z)^{-4}$ cosmological diminution of surface brightness. Since the observed X-ray jet structures have length scales of 10's of kpc projected on the sky, they will be at least several arcsec long at redshifts greater than 2, and would easily be resolved by Chandra. In fact, all objects intrinsically similar to PKS 0637-752, or the outer knots of 3C 273, would be bright enough to already be detected by *ROSAT*, but would appear as point sources to the resolution of the PSPC all-sky survey.

Where are these bright X-ray jets at high redshifts? They could not be recognized as extended in the *ROSAT* all sky survey, so they would most likely be identified simply as part of the quasar core emission. If the quasar itself were not recognized, e.g., because it was too faint, the jet could be among the miscellaneous unidentified sources. Alternately, the jet could outshine the quasar in X-rays, and be cataloged at a position some distance away from the quasar, and again be a miscellaneous unidentified source.

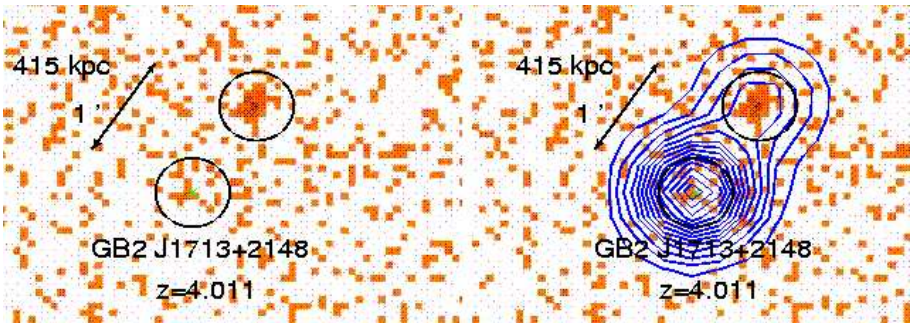

Fig. 12. Left panel shows a *ROSAT* HRI observation of the quasar GB 1713+2148 (green cross). The quasar is at most a 3σ detection in the $20''$ extraction circle. A stronger, unidentified source lies $\approx 1'$ to the NW. The right panel superposed the NVSS 1.4 GHz radio contours, clearly showing the connection of the stronger source to the quasar.

Figure 12 shows a possible example of the last case. In this *ROSAT* HRI pointed observation, there was only a possible 3σ detection of the quasar GB 1713+2148 (Vignali *et al.* (2003)). There is an obvious stronger, point source about 1 arcmin to the NW (left panel of Figure 12). When the NVSS 1.4 GHz image (Condon *et al.* (1998)) is superposed, we see the contours of the radio loud quasar extending around this source (Gurvits *et al.* (2003)), so that it is clearly associated with the quasar, at a redshift z=4.011 (Hook & McMahon (1998)). We still need a high resolution X-ray image to ascertain if this is really an X-ray jet, or perhaps just a hotspot or lobe.

Another case is due to Siemiginowska *et al.* (2003) (Figure 13). Here the X-ray image (left panel) is clearly extended, and the analysis in the central panel shows that the data (solid line) cannot be simulated simply by two point sources (dotted line). Cheung (2003) has analyzed archival VLA data, and found a coincident jet at 1.4 GHz (right panel). An IC/CMB analysis shows that this jet must be in relativistic motion, with a Doppler factor $\delta \geq 2.6$ and a magnetic field $B \leq 161 \mu G$, where the uncertainty is largely due to the uncertain slope of the radio and X-ray emission (Siemiginowska *et al.* (2003)).

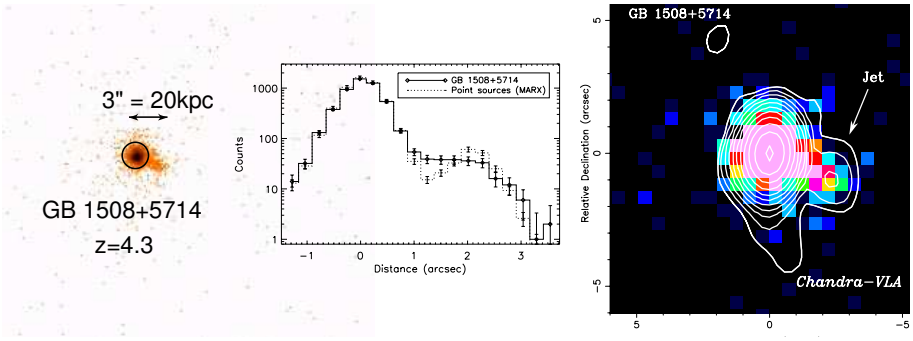

Fig. 13. Left and center from Siemiginowska *et al.* (2003): *Chandra* image binned in 0.″15 pixels, clearly showing extent to the WSW of the quasar. The circle is 2.″5 diameter, and contains 95% encircled power. The solid histogram is the intensity profile along the jet, which clearly cannot be simulated by two point sources (dotted histogram). Right: Cheung (2003) subsequently discovered a radio jet in archival 1.4 GHz VLA data.

5 Summary

We have reviewed some examples where X-ray and radio astronomy act in conjunction to reveal the workings of energy and matter outflow. Radio observations show the presence of magnetic fields, and allow calculations of *minimum* energy densities and total energy. X-ray observations can sometimes break the degeneracy between the magnetic field and particle densities and thus test the equipartition assumptions, although notably in the case of quasar jets the X-ray observations add a new parameter by revealing bulk relativistic motions. In the case of clusters of galaxies, the radio observations apparently have solved the problem of retarding the cooling flows in clusters of galaxies, while the energetics required by the X-ray data lead to an inference of much larger total energies being supplied by the central black hole.

Acknowledgements

This work was supported in part by NASA contract NAS8-39073 to the Chandra X-ray Center, and NASA grant GO2-3151C to SAO. This research used the NASA Astrophysics Data System Bibliographic Services, and the NASA/IPAC Ex-

tragalactic Database (NED) which is operated by the Jet Propulsion Laboratory, California Institute of Technology, under contract with the National Aeronautics and Space Administration.

References

Arnaud, K. A. 1988, in "Cooling flows in clusters and galaxies", Proceedings of the NATO Advanced Research Workshop, (Dordrecht: Kluwer Academic Publishers), 31

Atoyan, A., & Dermer, C. D. 2001, PRL, 22, 1102

Blanton, E. L., Sarazin, C. L., McNamara, B. R., & Wise, M. W. 2001, ApJ, 558, L15

Blundell, K. M., Kassim, N. E., & Perley, R. A. 2002, in Rao, A. P., Swarup, G., & Gopal-Krishna, eds., Proc IAU Coll. 199, "The Universe at Low Radio Frequencies," 189, (astro-ph/0004005)

Böhringer, H., Voges, W., Fabian, A. C., Edge, A. C., & Neumann, D. M. 1993, MNRAS, 264, L25

Bowyer, C. S., Lampton, M., Mack, J., & de Mendonca, F. S. 1971, ApJ, 161, L1

Bradt, H., Mayer, W., Naranan, S., Rappaport, S., & Spada, G. 1967, ApJ, 150, L199

Brunetti, G., Bondi, M., Comastri, A., & Setti, G. 2002, A& A, 381, 795

Burns, J. O. 1990, AJ, 99, 14

Celotti, A., Ghisellini, G., & Chiaberge, M. 2001, MNRAS, 321, L1.

Cheung, C. C. 2004, ApJ, 600, L23

Churazov, E., Forman, W., Jones, C., & Bhringer, H. 2000, A&A, 356, 788

Clarke, D. A., Harris, D. E., & Carilli, C. L. 1997, MNRAS, 284, 981

Condon, J. J., Cotton, W. D., Greisen, E. W., Yin, Q. F., Perley, R. A., Taylor, G. B., & Broderick, J. J. 1998, AJ, 115, 1693

Corbel, S. *et al.* 2002, Science, 298, 196

Dermer, C. D., & Schlickeiser, R. 1994, ApJS, 90, 945

De Young, D. S. 2003, MNRAS, 343, 719

Fabian, A. C. 1994, ARA&A, 32, 277

Fabian, A. C., et al. 2000, MNRAS, 318, L65.

Fabian, A. C., Celotti, A., Blundell, K. M., Kassim, N. E., & Perley, R. A. 2002, MNRAS, 331, 369

Fabian, A. C., Sanders, J. S., Allen, S. W., Crawford, C. S., Iwasawa, K., Johnstone, R. M., Schmidt, R. W., Taylor, G. B. 2003, MNRAS, 344, L43

Felten, J. E. & Morrison, P. 1966, ApJ, 146, 686

Flanagan, K. A., Canizares, C. R., Davis, D. S., Dewey, D., Houck, J. C., Schattenburg, M. L. 2000, Bull. AAS, 32, 725

Fredericks, A. C., Flanagan, K. A., Canizares, C. R., Dewey, D., Houck, J. C., Schattenburg, M. L. 2001, Bull. AAS, 33, 1491

Gaetz, T. J., Butt, Yousaf M., Edgar, Richard J., Eriksen, Kristoffer A., Plucinsky, Paul P., Schlegel, Eric M., Smith, Randall K. 2000, ApJ, 534, L47

Gaensler, B. M. 2003, in "Texas in Tuscany (XXI Symposium on Relativistic Astrophysics)," eds. R. Bandiera, R. Maiolino, F. Mannucci, (World Scientific: Singapore), 297

Ghisellini, G. & Celotti, A. 2001, MNRAS, 327, 743

Gurvits, Leonid I., Frey, Sandor, Mosoni, Laszlo, Garrington, Simon T., Garrett, Michael A., & Tsvetanov, Zlatan 2003, "Maps of the Cosmos," IAU Symposium 216

Hansen, L., Jørgenson, H. E., & Nørgaard-Nielson, H. U. 1995, A&A, 297, 13

Hardcastle, M. J., Birkinshaw, M., Cameron, R. A., Harris, D. E., Looney, L. W., & Worrall, D. M. 2002, ApJ, 581, 948

Hardcastle, M. J., Birkinshaw, M. & Worrall, D. M. 2001, MNRAS, 323, L17

Harris, D. E. et al. 2000, ApJ, 530, L81

Heinz, S., Reynolds, C. S., & Begelman, M. C. 1998, ApJ, 501,126

Helfand, D. J., Collins, B. F., & Gotthelf, E. V. 2003, ApJ, 582, 783

Hook, I. M., & McMahon, R. G. 1998, MNRAS, 294, L7

Kellogg, E., Pedelty, A. & Lyon, R. G. 2001, ApJ, 563, L151

Marshall, H. L. *et al.* 2001, ApJ, 549, L167

Marshall, H. L. *et al.* 2002, Bull. AAS, 34, 647

McNamara, B. R., 1995, ApJ, 443, 77

McNamara, B. R., *et al.* 2000, ApJ, 534, L135

McNamara, B. R., *et al.* 2001, ApJ, 562, L149

Meier, D. L. 2003, New Astronomy Reviews, 47, 667

Michel, F. C. 1969, ApJ, 157, 1183

Michel, F. C. 1969, ApJ, 158, 727

Nulsen, P.E.J., David, L.P, McNamara, B. R., Jones, C., Forman, W. R., & Wise, M. 2002, ApJ, 568, 163

Nulsen, P. 2003, in "The Riddle of Cooling Flows in Galaxies and Clusters of Galaxies," eds T.H. Reiprich, J.C. Kempner, N. Soker, http://www.astro.virginia.edu/coolflow, and astro-ph/0310195

Pavlov, G. G., Teter, M. A., Kargaltsev, O., & Sanwal, D. 2003, ApJ, 591,1157

Sambruna, R. *et al.* 2002, ApJ, 571, 206

Sanders, J. S., & Fabian, A. C. 2002, MNRAS, 331, 273

Schwartz, D. A. *et al.* 2000, ApJ, 540 L69

Schwartz, D. A. 2002, ApJ, 569, L23

Schwartz, D. A. *et al.* 2003, in "Galactic Nuclei: from Central Engine to Host Galaxy," eds.: S. Collin, F. Combes & I. Shlosman, ASP Conference Series, 290, 359

Schwartz, D. A. *et al.* 2003, New Astronomy Reviews, 47, 461

Siemiginowska, A. *et al.* 2003, ApJ, 598, L15

Sun, M., Jones, C., Murray, S. S., Allen, S. W., Fabian, A. C., & Edge, A. C. 2003, ApJ, 587, 619

Tavecchio, F. *et al.* 2000, ApJ, 544, L23

Taylor, G. B., Perley, R. A., Inoue, M., Kato, T., Tabara, H., & Aizu, K. 1990, ApJ, 360, 41

Tucker, W. H., & Rosner, R. 1983, ApJ, 267, 547

Vignali, C., Brandt, W. N., Schneider, D. P., Garmire, G. P., & Kaspi, S. 2003, AJ, 125, 418

Weisskopf, M. , *et al.* 2000, ApJ, 536, L81

White, D. A., Jones, C., & Forman, W. 1997, MNRAS, 292, 419
Wilson, A.S., Young, A.J., & Shopbell,P.L., 2000, Ap.J., 544, L27
Worrall, D. M., Birkinshaw, M., Hardcastle, M. J. 2001, MNRAS, 326, L7